Geophysical Research Letters

RESEARCH LETTER
10.1029/2021GL096986

Key Points:

- Large available magnetic energy per particle led to significant proton acceleration by reconnection in the near-Sun heliospheric current sheet (HCS) at 16 and 20 Rs
- Proton beams and strahl electron dropouts in separatrices are evidence for HCS being a source of energetic protons seen outside the HCS
- Energetic protons beams outside the HCS also exist without strahl electron dropouts. Their origin is unlikely to be the local HCS exhaust

Supporting Information:

Supporting Information may be found in the online version of this article.

Correspondence to:

T. D. Phan,
phan@ssl.berkeley.edu

Citation:

Phan, T. D., Verniero, J. L., Larson, D., Lavraud, B., Drake, J. F., Øieroset, M., et al. (2022). Parker Solar Probe observations of solar wind energetic proton beams produced by magnetic reconnection in the near-Sun heliospheric current sheet. *Geophysical Research Letters*, *49*, e2021GL096986. https://doi.org/10.1029/2021GL096986

Received 9 NOV 2021
Accepted 30 MAR 2022

Parker Solar Probe Observations of Solar Wind Energetic Proton Beams Produced by Magnetic Reconnection in the Near-Sun Heliospheric Current Sheet

T. D. Phan[1], J. L. Verniero[2], D. Larson[1], B. Lavraud[3,4], J. F. Drake[5], M. Øieroset[1], J. P. Eastwood[6], S. D. Bale[1,7], R. Livi[1], J. S. Halekas[8], P. L. Whittlesey[1], A. Rahmati[1], D. Stansby[9], M. Pulupa[1], R. J. MacDowall[2], P. A. Szabo[2], A. Koval[2,10], M. Desai[11], S. A. Fuselier[11], M. Velli[12], M. Hesse[13], P. S. Pyakurel[1], K. Maheshwari[1], J. C. Kasper[14], J. M. Stevens[15], A. W. Case[15], and N. E. Raouafi[16]

[1]SSL, University of California, Berkeley, CA, USA, [2]NASA Goddard Space Flight Center, Greenbelt, MD, USA, [3]Laboratoire d'Astrophysique de Bordeaux, University Bordeaux, Pessac, France, [4]IRAP, CNRS, CNES, Université de Toulouse, Toulouse, France, [5]University of Maryland, College Park, MD, USA, [6]The Blackett Laboratory, Imperial College London, London, UK, [7]Physics Department, University of California, Berkeley, CA, USA, [8]University of Iowa, Iowa City, IA, USA, [9]Mullard Space Science Laboratory, University College London, Dorking, UK, [10]University of Maryland, Baltimore County, Baltimore, MD, USA, [11]Southwest Research Institute, San Antonio, TX, USA, [12]University of California, Los Angeles, CA, USA, [13]NASA Ames Research Center, Moffett Field, CA, USA, [14]Climate and Space Sciences and Engineering, University of Michigan, Ann Arbor, MI, USA, [15]Smithsonian Astrophysical Observatory, Cambridge, MA, USA, [16]Johns Hopkins University Applied Physics Laboratory, Laurel, MD, USA

Abstract We report observations of reconnection exhausts in the Heliospheric Current Sheet (HCS) during Parker Solar Probe Encounters 08 and 07, at 16 R_s and 20 R_s, respectively. Heliospheric current sheet (HCS) reconnection accelerated protons to almost twice the solar wind speed and increased the proton core energy by a factor of ~3, due to the Alfvén speed being comparable to the solar wind flow speed at these near-Sun distances. Furthermore, protons were energized to super-thermal energies. During E08, energized protons were found to have leaked out of the exhaust along separatrix field lines, appearing as field-aligned energetic proton beams in a broad region outside the HCS. Concurrent dropouts of strahl electrons, indicating disconnection from the Sun, provide further evidence for the HCS being the source of the beams. Around the HCS in E07, there were also proton beams but without electron strahl dropouts, indicating that their origin was not the local HCS reconnection exhaust.

Plain Language Summary Magnetic reconnection in current sheets is a universal plasma process that converts magnetic energy into particle energy. The process is important in many laboratory, solar, and astrophysical plasmas. The heliospheric current sheet (HCS), which originates from the Sun and extends throughout the heliosphere, is the largest current sheet in the solar system. One of the surprises of the Parker Solar Probe mission is the finding that magnetic reconnection is almost always active in the near-Sun HCS, despite its enormous scales. In this paper, we report direct evidence showing that reconnection in the HCS close to the Sun can be a source of energetic protons observed in the solar wind. The reason protons can be accelerated to high energies (to tens of kilo-electronvolts) is because the available magnetic energy per particle is high close to the Sun. This finding is important because the source of energetic protons in the heliosphere is unknown.

1. Introduction

Magnetic reconnection converts magnetic energy into particle energies. In the solar wind at 1 AU, reconnection exhausts have been detected in Interplanetary Coronal Mass Ejections (ICME), in random solar wind current sheets, and occasionally in the heliospheric current sheet (HCS) (e.g., Gosling et al., 2005a, 2005b, 2006; Eriksson et al., 2009; Huttunen et al., 2008; Lavraud et al., 2009; Mistry et al., 2015; Phan et al., 2006; Ruffenach et al., 2012).

Commonly reported in-situ signatures of reconnection in solar wind current sheets include Alfvénic plasma jetting and heating (e.g., Drake et al., 2009; Gosling et al., 2005a; Phan et al., 2006). Kinetic signatures

such as counterstreaming ions have also been seen inside some solar wind exhausts (Gosling et al., 2005a; Lavraud et al., 2021), as have electron signatures of the separatrix layers bounding the exhaust (Gosling et al., 2005a, 2005b, 2006; Lavraud et al., 2009; Phan et al., 2021). Ion separatrix signatures in the form of proton beams have also been reported (Huttunen et al., 2008; Lavraud et al., 2021).

In the solar wind at 1 AU, the available magnetic energy per particle, $m_i V_A^2$ (Shay et al., 2014), is only ~25 eV (for a typical V_A~ 50 km/s), where m_i is proton mass and V_A the Alfvén speed. Thus, the energy increase associated with reconnection plasma jetting and bulk heating is small compared to the core solar wind flow energy of ~1 keV. Nevertheless, energetic ions up to MeV energies have been seen near some reconnecting current sheets at 1 AU (e.g., Khabarova et al., 2015; Khabarova & Zank, 2017). The open question is whether they originate from the local current sheet or at a site closer to the Sun, and whether they are associated with reconnection or other processes.

Parker Solar Probe (PSP) provides a unique opportunity to examine this question, since as its perihelion lowers, it samples the solar wind with increasing magnetic energy per particle, because of the higher Alfvén speed in the near-Sun solar wind. During the first several orbits, Parker Solar Probe (PSP) detected exhausts in current sheets associated with the heliospheric current sheet (HCS), Interplanetary Coronal Mass Ejections (ICMEs), magnetic flux ropes (Lavraud et al., 2020; Phan et al., 2020, 2021; Szabo et al., 2020), and at the boundaries of some magnetic "switchbacks" (Froment et al., 2021).

In this paper, we report Parker Solar Probe (PSP) observations of reconnection exhausts and surrounding regions during Encounters 08 and 07 (hereafter referred to as E08 and E07) crossings of the heliospheric current sheet (HCS).

2. Data and Coordinate System

We use four samples/s magnetic field data from the FIELDS fluxgate magnetometer (Bale et al., 2016) and 0.87 s-resolution proton data from the SWEAP/SPAN-ion instrument (Livi et al., 2020). We also use core electron temperature moments (Halekas et al., 2020), and pitch angle information of 314 eV electrons measured by the SWEAP/SPAN-electron instrument (Kasper et al., 2016; Whittlesey et al., 2020), and ISOIS/EPI-Lo (McComas et al., 2016) ion flux data obtained from double coincidence time-of-flight measurements, which may be susceptible to background counts from ultraviolet. We show SPAN proton temperature moments of the entire distribution, as well as core temperatures obtained from bi-Maxwellian fits of the core population (Stansby et al., 2018; Woodham et al., 2021).

For simplicity we display all data in RTN coordinates because the E07 and E08 HCS lay extremely close to the R-T plane (see in Supporting Information S1).

3. E08 HCS

We describe E08 before E07 because the HCS origin of the proton beams is clear in E08. The understanding of E08 raises questions about the source of proton beams seen in E07.

3.1. Overview

Figure 1 shows the PSP crossing of the HCS on 2021-04-29, at 08:14:23-08:28:16 UT (between the two black vertical dashed lines at "t_1" and "t_2"). The HCS crossing is recognized by the polarity change of B_R (Figure 1g) and switching of strahl electron pitch angle fluxes from 0° to 180° (Figure 1c) across the current sheet. The crossing occurred at perihelion, ~16 R_S from the Sun. The magnetic field strength was ~400 nT before the HCS crossing, and ~330 nT after. From 08:28:16 UT ("t_2") to 08:51:30 UT ("t_3"), PSP seemed to linger near the exhaust boundary while dipping occasionally back into the exhaust as suggested by several strahl dropouts (panels d and e) and radial velocity increases (panel h). Finally it reached the solar wind proper at "*t3*", where |**B**| reached close to its pre-HCS value of 400 nT. Thus, there are some uncertainties about the true location of the trailing edge of the HCS.

The field rotation across the HCS was 162°, and the HCS was bifurcated. The hybrid Alfvén speed (V_A) based on B_R and the proton mass density ρ on the two sides of the HCS, $V_{AR,hybrid} = [B_{R1}B_{R2}(B_{R1} + B_{R2})/\mu_0(\rho_1 B_{R2} + \rho_2 B_{R1})]^{0.5}$

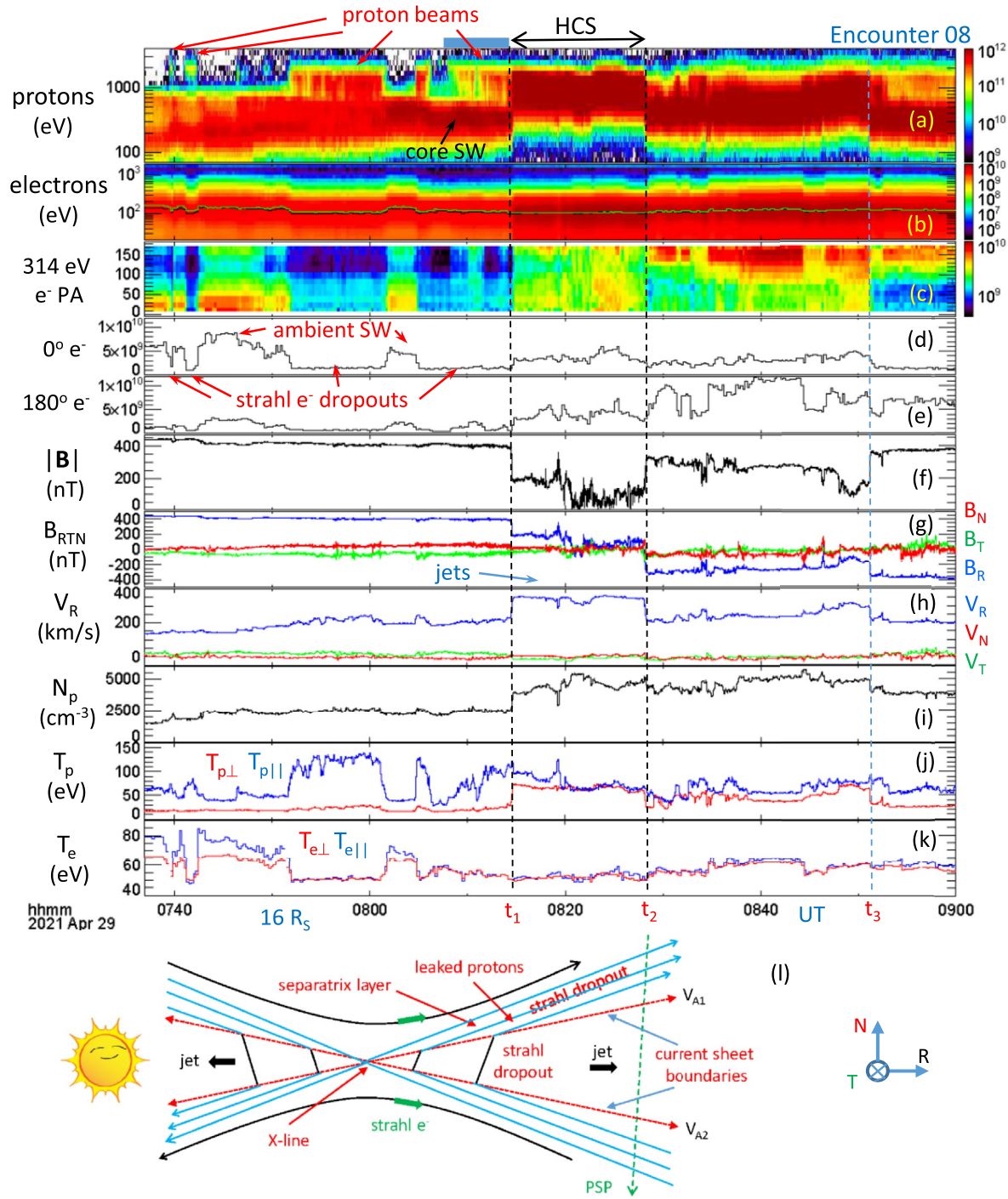

Figure 1. Parker Solar Probe (PSP) crossing of a reconnecting heliospheric current sheet (HCS) in E08. (a and b) proton and electron spectrograms in differential energy flux ($eVs^{-1}cm^{-2}ster^{-1}\ eV^{-1}$), (c) pitch angle distribution of 314 eV electrons, (d and e) differential energy fluxes of 314 eV electrons at 0°–30° and 150°–180° pitch angles, (f and g) magnetic field magnitude and components in RTN, (h and i) proton velocity and density, (j) proton temperature moment, (k) electron temperatures, and (l) schematic illustration of the standard reconnection exhaust and separatrix layers and the RTN coordinates. The vertical dashed lines mark the edges of the exhaust. The proton velocity is in the Sun's frame, while the spectrograms are in spacecraft frame. The PSP velocity in RTN at E08 perihelion was (−1,147, −4 km/s). The nearly indistinguishable black and green curves in panel (b) are twice the core T_e and the peak in differential energy fluxes.

(Cassak & Shay, 2007), was ~134 km/s. The proton and electron β were 0.15 and 0.32 prior to and 0.40 and 0.86 after the HCS crossing.

The HCS crossing duration (between "t_1" and "t_2") was ~833 s, which translates to an exhaust width of 1.8×10^4 km, or ~4,620 ion inertial lengths (d_i), based on the measured normal velocity of the current sheet relative to the spacecraft of ~21 km/s (not shown).

3.2. Proton Bulk Acceleration and Bulk Heating of the Core Population

Figure 1h shows that inside the current sheet there was a proton jet of ΔV_R ~140 km/s (relative to the external solar wind V_R of ~210 km/s). The opposite δV_R-δB_R correlations upon entry and exit of the HCS are consistent with reconnection (Gosling et al., 2005a). The jet speed was close to the hybrid V_A of 134 km/s, in close agreement with reconnection predictions. The positive ΔV_R jet implies that the X-line was located sunward of PSP (Figure 1l).

Also consistent with reconnection are density (Figure 1i) and core proton temperatures (Figure 2d) enhancements inside the exhaust. The ~50 eV average core proton bulk heating in this event is substantially higher than the 1–2 eV heating seen in previous HCS exhausts observed by PSP further (>29 R_s) away from the Sun (Phan et al., 2021). The larger heating is roughly consistent with the expectation from the scaling of reconnection proton heating with the available magnetic energy per particle, $\Delta T_i \propto m_i V_A^2$ (Drake et al., 2009; Haggerty et al., 2015; Phan et al., 2014). There was no clear evidence for electron heating (Figure 1k), although the heating may be hard to discern since the empirically expected heating is only ~3 eV for the given external V_A of ~134 km/s (Phan et al., 2013).

3.3. Ion and Electron Separatrix Signatures: Proton Beams and Strahl Electron Dropouts

As the solar wind protons were bulk accelerated by reconnection to 1.7 times the ambient solar wind speed (from 210 to 350 km/s), the solar wind proton core energy nearly tripled. The exhaust distributions (Figures 2i and 2j) were much broader than the core solar wind distributions outside the HCS (Figures 2g and 2h). Further, energization inside the exhaust significantly exceeds that expected from the standard picture of interpenetrating protons gaining twice the Alfvén speed (of 134 km/s) as they go through the magnetic kinks (Figure 2i). The tail of the proton spectra extended to 2.5 keV (Figure 1a) and could be higher but not measurable owing to insufficient SPAN geometric factor above that energy for the given fluxes. ISOIS/EPI-Lo data suggest the presence of ion intensity enhancements up to ~40 keV/nucleon in the exhaust and in the surrounding regions (Figure 2e). Thus, proton energization in the HCS must involve additional (e.g., multi X-line or other turbulent) acceleration mechanisms.

If the exhaust boundaries are magnetically open, energized protons with parallel speeds faster than the Alfvénic outflowing field line speed (~140 km/s in the solar wind frame, and ~350 km/s in the spacecraft frame) can escape the exhaust along separatrix field lines. Immediately outside and prior to the HCS, marked by the blue bar at the top of Figure 1, there were protons at higher energies (extending to at least 2.5 keV) than the core solar wind. Figure 2e shows that there were ions up to ~40 keV/nuc in this region. The following observational evidence points to the source being reconnection-energized protons that leaked/escaped from of the HCS:

1. The high-energy population outside the HCS had a similar high-energy spectrum profile as the reconnection-accelerated protons seen inside the HCS (Figure 1a).
2. In the blue-bar interval next to the HCS, there was a general trend of an energy dispersion of the low-energy cutoff of the high-energy population, with higher low-energy cutoff further away from the HCS (Figure 1a). The energy dispersion is consistent with velocity filter effects (Lavraud et al., 2002; Onsager et al., 1991): Leaked protons on separatrix field lines further from the current sheet had longer distances to travel, and could reach PSP only if they had sufficiently high energies. On separatrix field lines closer to the current sheet, protons with a broader range of energy could reach PSP. The crossing duration of the blue-bar interval was approximately half of the exhaust duration, consistent with the theoretical expectation of a separatrix layer ~half the exhaust width (Biskamp, 2000). The E08 separatrix layer was wide (~10^4 km, or ~2,300 d_i).

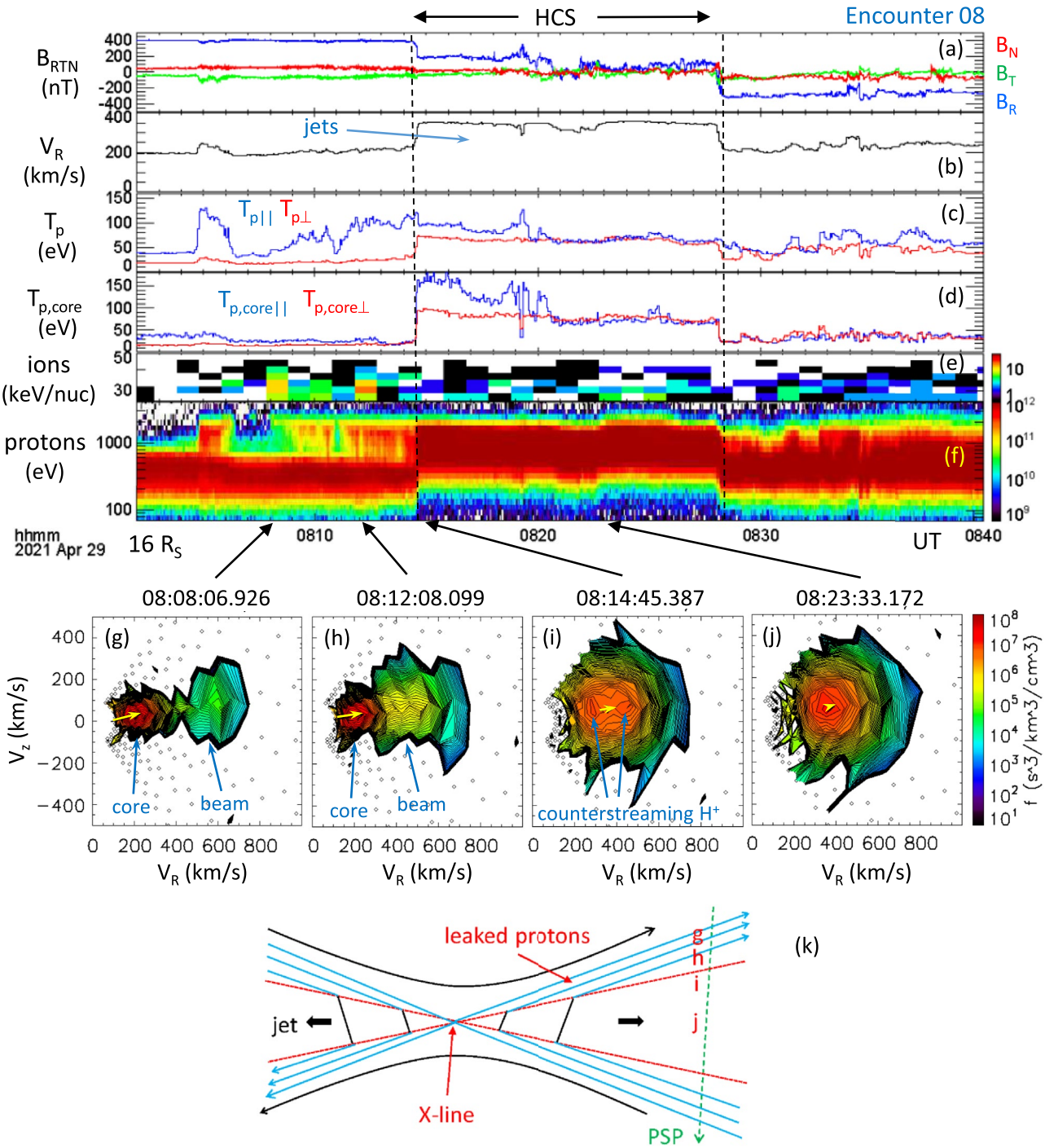

Figure 2. Proton distributions in and around the E08 heliospheric current sheet (HCS). (a) Magnetic field, (b–d) proton radial velocity, temperature moment, and core temperatures, (e) ion spectrogram from ISOIS/EPI-Lo, in counts/energy bin, and (f) proton spectrograms, (g–j) proton distributions summed and collapsed onto θ-plane in SPAN-ion instrument coordinates (Verniero et al., 2020): (g) near the outer edge of separatrix layer, (h) in the separatrix layer closer to the HCS, (i) in the exhaust, (j) in the weak |**B**| region of the exhaust, and (k) schematics showing the locations where the protons distributions g–j were sampled. The yellow arrow in panels g–j points along **B**, and its length represents the local V_A.

3. The presence of proton beams coincided with a significant drop in 0° 314 eV electron fluxes (Figures 1c and 1d) compared to the ambient solar wind, consistent with the beams being on separatrix field lines that are connected to an anti-sunward exhaust and disconnected from the Sun (Figure 1l) (Gosling et al., 2005b;

Lavraud et al., 2009). Further to the left of blue-bar interval, there were intermittent detections of proton beams (most likely associated with partial PSP re-entries into the separatrix layer due to HCS flapping motions). Remarkably, each occurrence of the beams coincided with strahl dropouts. Similar to previously reported anti-sunward reconnection exhausts with field line disconnection (Gosling et al., 2005b; Phan et al., 2021), 314 eV flux dropouts were not complete, possibly due to the presence of halo electrons in the ambient solar wind (Gosling et al., 2005b).

4. Proton velocity distribution function (VDF) measured in and adjacent to the HCS provide the clearest evidence that the leaked protons are the high-energy and field-aligned portion of the energized distributions in the exhaust. Figure 2i shows a velocity distribution function (VDF) inside the HCS close to the left edge. The velocity distribution function (VDF) was much broader than the core solar wind seen outside the current sheet (Figures 2g and 2h), and consisted (in the solar wind frame) of two field-aligned counterstreaming proton populations (Eastwood et al., 2018; Gosling et al., 2005a; Phan et al., 2007). The VDFs of the core population became more isotropic in the weak field region of the exhaust (Figure 2j). Outside the HCS, the VDFs (Figures 2g and 2h) consisted of a narrow (cold) core population and a higher energy anti-sunward (positive V_R) field-aligned beam (with V_R between ~300 and ~750 km/s). This is consistent with the escaping protons being the high-energy portion of the exhaust proton distributions that streamed faster than the reconnecting field-line speed. Further from the HCS the leaked population consists of only the highest velocities and looks "detached" from the core (Figure 2g), while closer to the HCS (Figure 2h), a larger range of velocities is seen.

While the ion and electron separatrix signatures were clear on the side prior to the HCS, they were much less clear after the HCS, partly because of the uncertainly about the location of the trailing edge of the HCS. If the trailing edge was at "t_2" (Figure 1), the absence of proton beams (Figure 1a) and 180° 314 eV electron dropouts (Figures 1c and 1e) would imply a lack of a separatrix layer after the HCS, a result that is not consistent with traditional 2D models of reconnection exhausts. If the trailing edge was at "t_3", there were proton beams to the right of the boundary, but no velocity filter signatures were apparent. There were the expected simultaneous dropouts of strahl electron immediately after "t_3", but no strahl dropouts in much of the region with proton beams after that. The presence of proton beams without concurrent strahl dropouts occurred more clearly outside an E07 HCS, which we will discuss next in more details.

4. E07 HCS

In contrast to the E08 HCS described above, we now describe an event in which energetic proton beams observed adjacent to the HCS do not appear to originate from the HCS reconnection exhaust.

4.1. Overview

Figure 3 shows a crossing of the HCS during E07 at 20 R_S, with B_R reversal (Figure 3g) and concurrent switching of strahl electron pitch angle fluxes from predominantly 0° to 180° (Figure 3c). The field rotation across the HCS was 170°. The HCS was bifurcated, with sharp B_R changes at the two edges and a plateau in between (Figure 3g). The plateau was above zero and the magnetic shear was small at the leading edge due to the higher propagation speed of an Alfvénic magnetic kink at the leading edge (because of the higher V_A there compared to the trailing edge). The non-zero B_R of the plateau is represented by the slanted (black) field lines inside the exhaust in Figure 4m. The proton and electron β were 0.25 and 0.53 before and 0.44 and 0.83 after the HCS.

The HCS crossing duration was ~1020 s. With a measured current sheet normal velocity relative to the spacecraft of ~39 km/s, the current sheet width was ~4×10^4 km, or ~8,530 d_i.

4.2. Proton Bulk Acceleration and Heating

Proton V_R jetting was observed inside the HCS (Figure 3h). The jet speed was remarkably steady and laminar throughout most of the HCS. V_R was more variable in the last 3 min before the exit of the HCS where there were multiple bipolar variations of B_N which could indicate the presence of magnetic flux ropes (Eastwood et al., 2021). The V_R jet speed (relative to the adjacent solar wind flow) was ~+125 km/s, close to the hybrid V_A

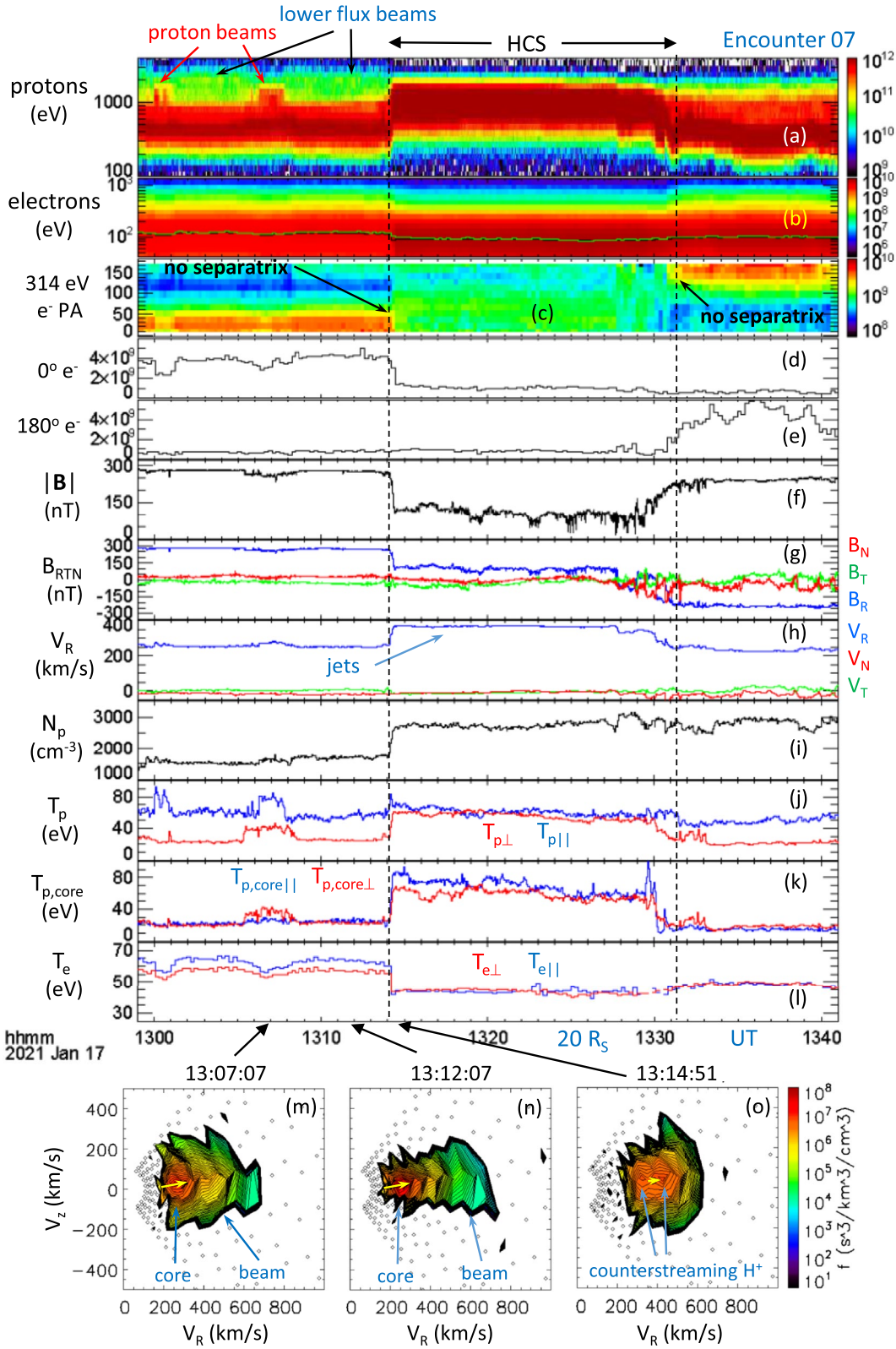

Figure 3. PSP crossing of a reconnecting heliospheric current sheet (HCS) in E07. The parameters are the same as in Figures 1 and 2. Velocity distribution functions (VDFs) in (m and n) were sampled outside the HCS, and VDF (o) was sampled inside the HCS near the left edge.

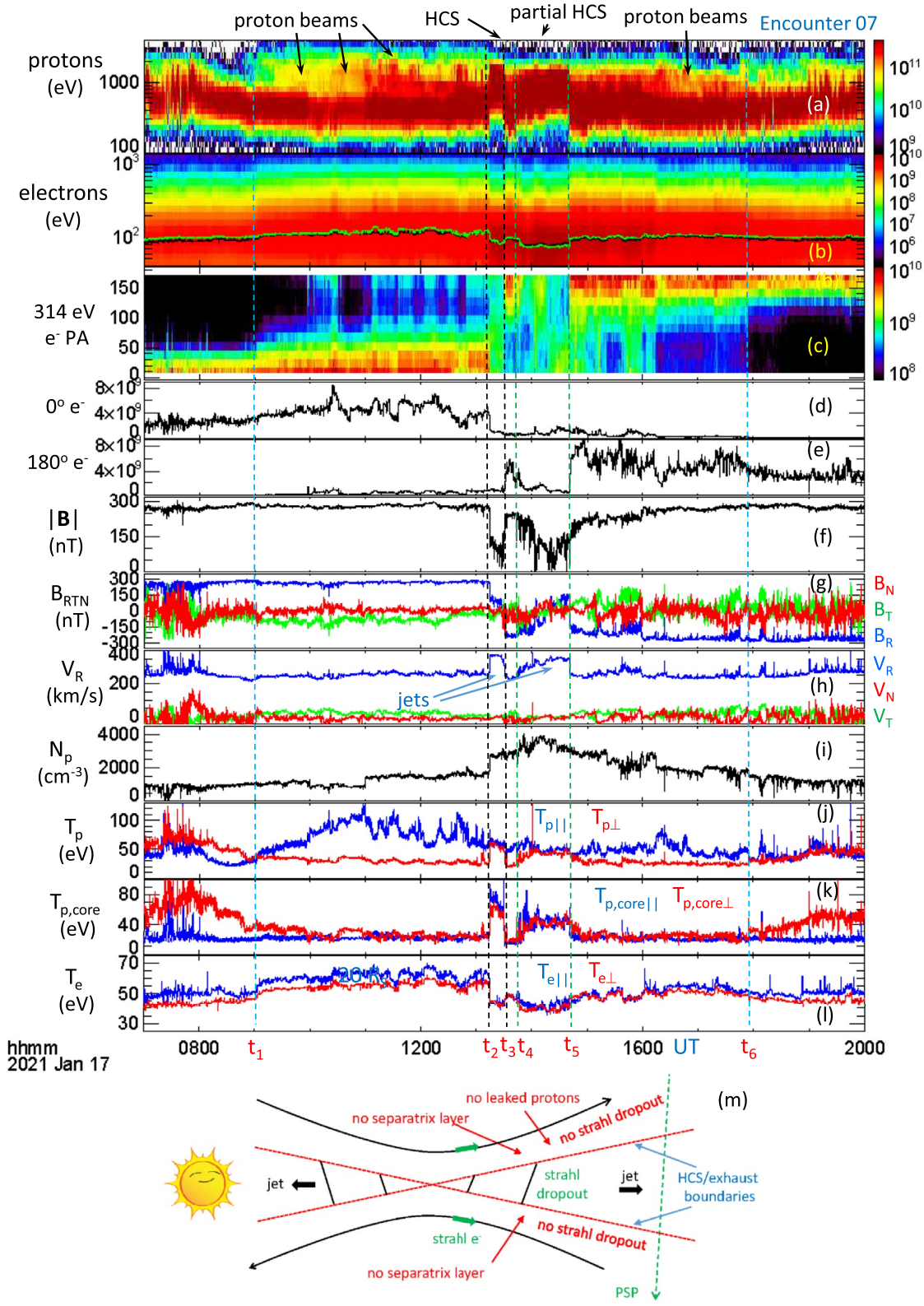

Figure 4. Zoom-out of Figure 3. The black dashed lines mark the edges of the complete HCS crossing. The interval between the two green lines is a partial HCS crossing. The blue dashed lines mark the outer boundaries of the regions surrounding the HCS that showed persistent $T_{p\|} > T_{p\perp}$. The sketch in (m) shows a 2D exhaust without separatrix layers. It is unphysical because the black field lines end at the exhaust boundaries in a non-physical way.

of 120 km/s based on B_R ~280 nT and N_p ~1,720 cm^{-3} prior to HCS, and B_R ~-240 nT and N_p~2,550 cm^{-3} after. The Alfvénic jetting is therefore consistent with reconnection. The anti-sunward jet indicates an X-line located sunward of PSP. Counterstreaming proton populations were present in more than half of the exhaust (Figure 3o).

There was density compression (Figure 3i) and a ~40 eV average core proton temperature increase (Figure 3k) inside the exhaust, consistent with reconnection expectations. However, the core T_e decreased within the exhaust (Figure 3l). This decrease is confirmed by a shift to lower energy of the peak in electron differential energy fluxes, as shown by the green curve in Figure 3b. The reduction in T_e in the exhaust is not an expected signature of reconnection (Pulupa et al., 2014) and is currently not understood.

4.3. Proton Beams Outside the HCS and the Lack of Strahl Electron Dropouts

The enhanced proton flow speed and heating inside the exhaust resulted in a shift to higher energies of the core protons by about a factor of three compared to the core solar wind outside the HCS (Figure 3a), and the exhaust distributions (Figure 3o) are much broader than the core solar wind outside the HCS (Figures 3m and 3n).

Prior to the HCS crossing, there were bursts of anti-sunward and field-aligned energetic proton beams (Figures 3a and 3m), resulting in $T_{p\|}$ moment enhancements. The large moment $T_{p\|}$ is due to a mixture of the core solar wind and field-aligned beams (Figure 3j), not parallel heating of the core population (Figure 3k). Slight drops in the fluxes of the 314 eV field-aligned strahl electrons were observed in conjunction with these proton beams (Figures 3c and 3d), but the drops were not significant compared to those discussed for the E08 separatrix layers.

On both sides of the HCS, 314 eV electrons (Figures 3b–3e) were present all the way to the edge of the current sheet, indicating the absence of a separatrix layer (Gosling et al., 2005b; Phan et al., 2021). Immediately outside the HCS on both sides, VDFs (Figure 3n) reveals the presence of anti-sunward beams, albeit at low fluxes. The upper energy of the low-flux beams on the left side of the HCS is higher than the exhaust population, suggesting that they did not leak out of the local exhaust. The lack of leaked proton beams, coupled with no electron separatrix signatures, indicate the absence of separatrix layers outside the exhaust. This, is not consistent with conventional 2D reconnection models.

Zooming out, Figure 4 shows a broad region around the full and partial crossings of the HCS. Energetic proton beams (panel a) and associated temperature moment anisotropy $T_{p\|} >> T_{p\perp}$ (Figure 4j) were present over a very broad region surrounding the HCS, extending all the way to the two blue dashed lines ("t_1" and "t_6") in Figure 4. The ISOIS/EPI-Lo instrument detected ion intensity enhancements up to ~50 keV/nucleon throughout the broad region with proton beams (Desai et al., 2022). The appearance of proton beams in the vicinity of the HCS suggests that the source was close to the HCS, or the HCS itself. However, in contrast to E08, there were essentially no dropouts of 314 eV electrons when the proton beams were observed. If these 314 eV electrons are strahl electrons from the Sun, their presence means that these field lines are connected to the Sun. This is inconsistent with the region being magnetically connected to an anti-sunward exhaust.

There may, however, be a different interpretation of the origin of the 314 eV electrons close to the E07 HCS. Figure 4b shows that there was an abrupt increase in the upper electron energy, increase of 0° and 180° fluxes (Figures 4d and 4e), and a sudden broadening of the 314 eV electron pitch angle (Figure 4c) across "t_1" and "t_6" (going toward the HCS from both sides), which mark where the temperature moment became persistently anisotropic $T_{p\|} >> T_{p\perp}$ (Figure 4j) due to the presence of proton beams. This suggests that the electrons with broader pitch-angle distributions adjacent to the HCS came from a different source than the narrower pitch-angle distributed electrons seen further away. The latter could be the usual strahls from the solar corona. The concurrent presence of the proton beams and the broad pitch-angle electrons suggests that they both originated from a common source sunward of PSP but close to the HCS. The source, however, cannot be the local HCS because the fluxes of 314 eV electrons inside the HCS were much lower than outside (Figures 3b–3e).

Could the 314 eV electrons and the energetic proton beams have leaked out along separatrix field lines of the HCS exhaust at a location closer to the Sun during active reconnection? In the traditional 2D steady-state picture, this is unlikely because the energetic particles would arrive at the PSP altitude at some distance from the exhaust boundaries. One would therefore expect a gap of 314 eV fluxes and proton beams next to the exhaust boundaries, but no gaps were observed.

5. Summary and Discussion

During E07 and E08, PSP encountered the HCS near perihelia. The HCS was bifurcated and displayed classic signatures of reconnection exhausts with Alfvénic outflows bounded by sharp slow-shock-like exhaust edges (Petschek, 1964), and counterstreaming protons suggestive of active reconnection with plasma entry across the local exhaust boundaries (Gosling et al., 2005a). At $16R_s$ (E08) and $20R_s$ (E07), the Alfvén speed of the solar wind was comparable to the solar wind flow speed. As a result, the proton energy gained through reconnection bulk acceleration was ∼3 times that of the surrounding solar wind energy, making the exhaust proton population clearly distinguishable from the ambient solar wind population. Further, protons were energized well beyond what is expected from an Alfvénic counterstreaming picture.

For E08, this has allowed the identification of protons leaking out of the local reconnecting HCS along separatrix field lines (that penetrate the exhaust boundary). The leaked protons appeared as energetic proton beams separated from the core solar wind when detected far from the HCS. Similar distributions have been reported by Verniero et al. (2020), although it is not clear how far away from the HCS those observations were. The interpretation of leaked proton beams is supported by the concurrent dropouts of strahl electrons, consistent with the spacecraft sampling the separatrix layer of an anti-sunward exhaust magnetically disconnected from the Sun.

For E07, energetic proton beams were observed in broad regions surrounding the HCS. However, in contrast to E08, there were no dropouts of 314 eV electrons associated with most proton beams, which could mean the absence of separatrix layers, and that the source of proton beams was not the local HCS exhaust. The true source of proton beams adjacent to the E07 HCS is not known.

The lack of separatrices adjacent to the E07 HCS exhaust (implying closed exhaust boundaries) is puzzling. The presence of counterstreaming protons in the exhaust, coupled with the fact that the velocity of the plasma jets was very close to the local external Alfvén speed, is usually taken as evidence for active reconnection with plasma entry across the local open exhaust boundaries (Gosling et al., 2005a). This apparent major contradiction with conventional 2D reconnection models is not understood.

HCS exhausts without separatrix layers are surprisingly common, both at 1 AU (Gosling et al., 2005b, 2006; Lavraud et al., 2009) and near the Sun (Phan et al., 2021). Future studies should investigate whether they could be associated with reconnection being intermittent or patchy (i.e., finite X-line), or when the HCS contains multiple active and non-active X-lines/flux ropes (Gosling et al., 1995; Khabarova et al., 2015; Lavraud et al., 2020; Réville et al., 2020; Shepherd et al., 2017).

In conclusion, PSP observations (e.g., E08) have shown that reconnection in the near-Sun HCS can produce high-energy protons seen adjacent to the HCS. The leaked proton beam energy is simply related to the energy of the accelerated protons inside the exhaust, which in turn depends on the available magnetic energy per particle in the local solar wind. Thus, reconnection in the near-Sun HCS energizes protons to much higher energies than at 1 AU. Further PSP observations closer to the Sun will shed more light on the relationship between reconnection and energetic protons in the solar wind.

Data Availability Statement

Data source: http://fields.ssl.berkeley.edu/data/, http://sweap.cfa.harvard.edu/pub/data/sci/sweap/, and https://spp-isois.sr.unh.edu/data_public/EPILo/level2/.

Acknowledgments
The authors are grateful for the dedicated efforts of the entire PSP team.

References

Bale, S. D., Goetz, K., Harvey, P. R., Turin, P., Bonnell, J. W., Dudok de Wit, T., et al. (2016). The FIELDS instrument suite for solar Probe plus. *Space Science Reviews*, *204*(1), 49–82. https://doi.org/10.1007/s11214-016-0244-5

Biskamp, D. (2000). Magnetic reconnection in plasmas *Cambridge monographs on plasma physics* (Vol. 3).

Cassak, P. A., & Shay, M. A. (2007). Scaling of asymmetric magnetic reconnection: General theory and collisional simulations. *Physics of Plasmas*, *14*(10), 102114. https://doi.org/10.1063/1.2795630

Desai, M. I., Mitchell, D. G., McComas, D. J., Drake, J. F., Phan, T., Szalay, J. R., et al. (2022). Suprathermal ion energy spectra and anisotropies near the heliospheric current sheet crossing observed by the parker solar Probe during encounter 7. *Acta Pathologica Japonica*, *927*(1), 62. https://doi.org/10.48550/arXiv.2111.00954

Drake, J. F., Swisdak, M., Phan, T. D., Cassak, P. A., Shay, M. A., Lepri, S. T., et al. (2009). Ion heating resulting from pickup in magnetic reconnection exhausts. *Journal of Geophysical Research*, *114*, 5111. https://doi.org/10.1029/2008JA013701

Eastwood, J. P., Mistry, R., Phan, T. D., Schwartz, S. J., Ergun, R. E., Drake, J. F., et al. (2018). Guide field reconnection: Exhaust structure and heating. *Geophysical Research Letters*, *45*, 4569–4577. https://doi.org/10.1029/2018GL077670

Eastwood, J. P., Stawarz, J. E., Phan, T. D., Laker, R., Robertson, S., Zhao, L. L., et al. (2021). Solar Orbiter observations of an ion-scale flux rope confined to a bifurcated solar wind current sheet. *Astronomy & Astrophysics*, *656*, A27. https://doi.org/10.1051/0004-6361/202140949

Eriksson, S., Gosling, J. T., Phan, T. D., Blush, L. M., Simunac, K. D. C., Krauss-Varban, D., et al. (2009). Asymmetric shear flow effects on magnetic field configuration within oppositely directed solar wind reconnection exhausts. *Journal of Geophysical Research*, *114*, A07103. https://doi.org/10.1029/2008ja013990

Froment, C., Krasnoselskikh, V., Dudok de Wit, T., Agapitov, O., Fargette, N., Lavraud, B., et al. (2021). Direct evidence for magnetic reconnection at the boundaries. *Astronomy & Astrophysics*, *650*, A5. https://doi.org/10.1051/0004-6361/202039806

Gosling, J. T., Birn, J., & Hesse, M. (1995). Three-dimensional magnetic reconnection and the magnetic topology of coronal mass ejection events. *Geophysical Research Letters*, *22*(8), 869–872. https://doi.org/10.1029/95gl00270

Gosling, J. T., McComas, D., Skoug, R., & Smith, C. (2006). Magnetic reconnection at the heliospheric current sheet and the formation of closed magnetic field lines in the solar wind. *Geophysical Research Letters*, *33*, L17102. https://doi.org/10.1029/2006GL027188

Gosling, J. T., Skoug, R. M., McComas, D. J., & Smith, C. W. (2005a). Direct evidence for magnetic reconnection in the solar wind near 1 AU. *Journal of Geophysical Research*, *110*, A01107. https://doi.org/10.1029/2004JA010809

Gosling, J. T., Skoug, R. M., McComas, D. J., & Smith, C. W. (2005b). Magnetic disconnection from the Sun: Observations of a reconnection exhaust in the solar wind at the heliospheric current sheet. *Geophysical Research Letters*, *32*, L05105. https://doi.org/10.1029/2005GL022406

Haggerty, C. C., Shay, M. A., Drake, J. F., Phan, T. D., & McHugh, C. T. (2015). The competition of electron and ion heating during magnetic reconnection. *Geophysical Research Letters*, *42*, 9657–9665. https://doi.org/10.1002/2015GL065961

Halekas, J. S., Whittlesey, P., Larson, D. E., McGinnis, D., Maksimovic, M., Berthomier, M., et al. (2020). Electrons in the young solar wind: First results from the parker solar Probe. *The Astrophysical Journal Supplement Series*, *246*(2), 22. https://doi.org/10.3847/1538-4365/ab4cec

Huttunen, K. E. J., Bale, S. D., & Salem, C. (2008). Wind observations of low energy particles within a solar wind reconnection region. *Annales Geophysicae*, *26*(6), 2701–2710. https://doi.org/10.5194/angeo-26-2701-2008

Kasper, J. C., Abiad, R., Austin, G., Balat-Pichelin, M., Bale, S. D., Belcher, J. W., et al. (2016). Solar wind electrons alphas and protons (SWEAP) investigation: Design of the solar wind and coronal plasma instrument suite for solar Probe plus. *Space Science Reviews*, *204*(1), 131–186. https://doi.org/10.1007/s11214-015-0206-3

Khabarova, O., Zank, G., Li, G., Le Roux, J. A., Webb, G. M., Dosch, A., & Malandraki, O. E. (2015). Small-scale magnetic islands in the solar wind and their role in particle acceleration. I. Dynamics of magnetic islands near the heliospheric current sheet. *Acta Pathologica Japonica*, *808*(2), 181. https://doi.org/10.1088/0004-637X/808/2/181

Khabarova, O. V., & Zank, G. P. (2017). Energetic Particles of keV–MeV Energies Observed near Reconnecting Current Sheets at 1 au. *Acta Pathologica Japonica*, *843*(1), 4. https://doi.org/10.3847/1538-4357/aa7686

Lavraud, B., Dunlop, M. W., Phan, T. D., Reme, H., Bosqued, J. M., Dandouras, I., et al. (2002). Cluster observations of the exterior cusp and its surrounding boundaries under northward IMF. *Geophysical Research Letters*, *29*, 1–4. https://doi.org/10.1029/2002GL015464

Lavraud, B., Fargette, N., Reville, N., Szabo, A., Huang, J., Rouillard, A. P., et al. (2020). The heliospheric current sheet and plasma shee during parker solar probe's first orbit. *The Astrophysical journal letters*, *894*(2), L19. https://doi.org/10.3847/2041-8213/ab8d2d

Lavraud, B., Gosling, J. T., Rouillard, A. P., Fedorov, A., Opitz, A., Sauvaud, J. A., et al. (2009). Observation of a complex solar wind reconnection exhaust from spacecraft separated by over 1800 R_E. *Solar Physics*, *256*(1), 379–392. https://doi.org/10.1007/s11207-009-9341-x

Lavraud, B., Kieokaew, R., Fargette, N., Louarn, P., Fedorov, A., Andre, N., et al. (2021). Magnetic reconnection as a mechanism to produce multiple proton populations and beams locally in the solar wind. *Astronomy & Astrophysics*, *656*, A37. https://doi.org/10.1051/0004-6361/202141149

Livi, R., Larson, D. E., Kasper, J. C., Abiad, R., Case, A. W., Klein, K. G., et al. (2020). The solar Probe ANalyzer - Ions on parker solar Probe. *The Astrophysical Journal Supplement Series*. https://doi.org/10.1002/essoar.10508651.1

McComas, D. J., Alexander, N., Angold, N., Bale, S., Beebe, C., Birdwell, B., et al. (2016). Integrated science investigation of the Sun (ISIS): Design of the energetic particle investigation. *Space Science Reviews*, *204*(1), 187–256. https://doi.org/10.1007/s11214-014-0059-1

Mistry, R., Eastwood, J. P., Phan, T. D., & Hietala, H. (2015). Development of bifurcated current sheets in solar wind reconnection exhausts. *Geophysical Research Letters*, *42*, 10–513. https://doi.org/10.1002/2015GL066820

Onsager, T. G., Thomsen, M. F., Elphic, R. C., & Gosling, J. T. (1991). Model of electron and ion distributions in the plasma sheet boundary layer. *Journal of Geophysical Research*, *96*, A12. https://doi.org/10.1029/91ja01983

Petschek, H. E. (1964). Magnetic field annihilation. In W. N.Hess (Ed.), *Proceedings of the AAS-NASA symposium* (Vol. 50, pp. 425). National Aeronautics and Space Administration, Science and Technical Information Division.

Phan, T. D., Bale, S. D., Eastwood, J. P., Lavraud, B., Drake, J. F., Oieroset, M., et al. (2020). Parker solar Probe in situ observations of magnetic reconnection exhausts during encounter 1. *The Astrophysical Journal Supplement Series*, *246*(2), 34. https://doi.org/10.3847/1538-4365/ab55ee

Phan, T. D., Drake, J. F., Shay, M. A., Gosling, J. T., Paschmann, G., Eastwood, J. P., et al. (2014). Ion bulk heating in magnetic reconnection exhausts at Earth's magnetopause: Dependence on the inflow Alfvén speed and magnetic shear angle. *Geophysical Research Letters*, *41*, 7002–7010. https://doi.org/10.1002/2014GL061547

Phan, T. D., Gosling, J. T., Davis, M. S., Skoug, R. M., Oieroset, M., Lin, R. P., et al. (2006). A magnetic reconnection X-line extending more than 390 Earth radii in the solar wind. *Nature*, *439*(7073), 175–178. https://doi.org/10.1038/nature04393

Phan, T. D., Lavraud, B., Halekas, J. S., Oieroset, M., Drake, J. F., Eastwood, J. P., et al. (2021). Prevalence of magnetic reconnection in the near-Sun heliospheric current sheet. *Astronomy & Astrophysics*, *650*, A13. https://doi.org/10.1051/0004-6361/202039863

Phan, T. D., Paschmann, G., Twitty, C., Mozer, F. S., Gosling, J. T., Eastwood, J. P., et al. (2007). Evidence for magnetic reconnection initiated in the magnetosheath. *Geophysical Research Letters*, *34*, 14. https://doi.org/10.1029/2007GL030343

Phan, T. D., Shay, M. A., Gosling, J. T., Fujimoto, M., Drake, J. F., Paschmann, G., et al. (2013). Electron bulk heating in magnetic reconnection at Earth's magnetopause: Dependence on inflow Alfvén speed and magnetic shear. *Geophysical Research Letters*, *40*, 4475–4480. https://doi.org/10.1002/grl.50917

Pulupa, M. P., Salem, C., Phan, T. D., Gosling, J. T., & Bale, S. D. (2014). Core electron heating in solar wind reconnection exhausts. *The Astrophysical Journal Letters*, *791*(1), L17. https://doi.org/10.1088/2041-8205/791/1/L17

Réville, V., Velli, M., Rouillard, A. P., Lavraud, B., Tenerani, A., Shi, C., & Strugarek, A. (2020). Tearing instability and periodic density perturbations in the slow solar wind. *The Astrophysical Journal Letters*, *895*, 1. https://doi.org/10.3847/2041-8213/ab911d

Ruffenach, A., Lavraud, B., Owens, M. J., Sauvaud, J. A., Savani, N. P., Rouillard, A. P., et al. (2012). Multispacecraft observation of magnetic cloud erosion by magnetic reconnection during propagation. *Journal of Geophysical Research*, *117*, A09101. https://doi.org/10.1029/2012JA017624

Shay, M. A., Haggerty, C. C., Phan, T. D., Drake, J. F., Cassak, P. A., Wu, P., et al. (2014). Electron heating during magnetic reconnection: A simulation scaling study. *Physics of Plasmas*, *21*(12), 122902. https://doi.org/10.1063/1.4904203

Shepherd, L. S., Cassak, P. A., Drake, J. F., Gosling, J. T., Phan, T. D., & Shay, M. A. (2017). Structure of exhausts in magnetic reconnection with an X-line of finite extent. *Acta Pathologica Japonica*, *848*(2), 90. https://doi.org/10.3847/1538-4357/aa9066

Stansby, D., Salem, C., Matteini, L., & Horbury, T. (2018). A new inner heliosphere proton parameter dataset from the Helios mission. *Solar Physics*, *293*(11), 155. https://doi.org/10.1007/s11207-018-1377-3

Szabo, A., Larson, D. E., Whittlesey, P., Stevens, M. L., Lavraud, B., Phan, T., et al. (2020). The heliospheric current sheet in the inner heliosphere observed by the parker solar Probe. *The Astrophysical Journal Supplement Series*, *246*(2), 47. https://doi.org/10.3847/1538-4365/ab5dac

Verniero, J. L., Larson, D. E., Livi, R., Rahmati, A., McManus, M. D., Pyakurel, P. S., et al. (2020). Parker solar Probe observations of proton beams simultaneous with ion-scale waves. *The Astrophysical Journal Supplement Series*, *248*(1), 5. https://doi.org/10.3847/1538-4365/ab86af

Whittlesey, P. L., Larson, D. E., Kasper, J. C., Halekas, J., Abatcha, M., Abiad, R., et al. (2020). The solar Probe ANalyzers—Electrons on the parker solar Probe. *The Astrophysical Journal Supplement Series*, *246*(2), 74. https://doi.org/10.3847/1538-4365/ab7370

Woodham, L. D., Horbury, T. S., Matteini, L., Woolley, T., Laker, R., Bale, S. D., et al. (2021). Enhanced proton parallel temperature inside patches of switchbacks in the inner heliosphere. *Astronomy & Astrophysics*, *650*, L1. https://doi.org/10.1051/0004-6361/202039415

Reference From the Supporting Information

Sonnerup, B. U. Ö., & Cahill, L. J., Jr. (1967). Magnetopause structure and attitude from Explorer 12 observations. *Journal of Geophysical Research*, *72*(1), 171. https://doi.org/10.1029/jz072i001p00171